# Phototransformation and Dark Reversion of Phytochrome in Deuterium Oxide†

Hemanta K. Sarkar and Pill-Soon Song*

ABSTRACT: The photostationary equilibrium between the Pr and Pfr forms of phytochrome shows a strong solvent deuterium isotope effect. Phytochrome transformation from the Pr to the Pfr form exhibits a small deuterium isotope effect, in Tris-$D_2O$ upon irradiation with red light, only after a photocycling of the phytochrome. In contrast, both the photoreversion and dark reversion of Pfr show an enhanced rate in $D_2O$. In addition to the shift in the photostationary equilibrium in $D_2O$, another pronounced effect of $D_2O$ on phytochrome is reflected in a significant enhancement of the fluorescence quantum yield of phytochrome (Pr). This result is interpreted in terms of the primary reaction involving an intramolecular proton transfer and its consequence in the phototransformation of phytochrome. It is further proposed that a tyrosyl residue acts as a general acid catalyst in the Pr to Pfr phototransformation, which is slower in $D_2O$ than in $H_2O$. The $D_2O$ solvent isotope effect on the photoreversion and dark reversion of Pfr is explained on the basis of acid catalysis, probably a specific acid catalysis by deuteronium ion.

Phytochrome, which triggers diverse photomorphogenic processes in plants by acting as a primary photoreceptor, can be phototransformed from its physiologically inactive Pr form to the active Pfr form and vice versa according to [see the most recent review by Rüdiger (1980)]

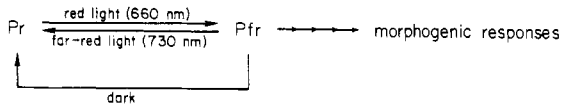


Elucidation of the chemical mechanism of phytochrome transformation depicted in the above scheme is crucial in understanding the molecular basis of primary events such as Pfr–receptor interactions in the photomorphogenic responses of plants, but it still remains to be established. The chromophore structure of the Pr form is now known with certainty (Klein & Rüdiger, 1978; Lagarias & Rapoport, 1980). However, the chromophore structure in the native Pfr form has not been determined. This situation is likely to remain for some time, as the thermal instability of the Pfr chromophore presents an almost insurmountable obstacle in its chemical structure determination (cf. scheme shown above). On the basis of spectroscopic characterization of phytochrome molecules, a molecular model has been proposed to elucidate the mechanism for the phototransformation (Song et al., 1979; Song, 1980; Hahn & Song, 1981), as illustrated in Figure 1.

According to this model, the rate-determining step in a Pr → Pfr phototransformation involves a C–H bond breaking at ring A, which follows an excited-state proton transfer from the ring A nitrogen to the ring C nitrogen as a result of an increase in $pK_a$ ($=pK_a^*$) in the latter (Song & Chae, 1979). Given that this mechanism is correct, we would expect the rate ($k_1$) of the first Pr → Pfr phototransformation cycle in $D_2O$ to be faster than the rates in subsequent cycles; the successive cycling enhances H–D exchange by exposing the tightly held Pr chromophore (Hahn et al., 1980); thus $k_1 > k_2 > k_3$, etc.

$$\mathrm{Pr} \xrightarrow[k_1]{660\ \mathrm{nm}} \mathrm{Pfr} \xrightarrow[k_{-1}]{730\ \mathrm{nm}} \mathrm{Pr} \xrightarrow[k_2]{660\ \mathrm{nm}} \mathrm{Pfr} \xrightarrow[k_{-2}]{730\ \mathrm{nm}} \mathrm{Pr} \xrightarrow[k_3]{660\ \mathrm{nm}}$$

$$\mathrm{Pfr} \xrightarrow[k_{-3}]{730\ \mathrm{nm}} \mathrm{Pr}, \text{ etc.}$$

In the course of assessing the above prediction, it was found that the absorption spectrum of Pfr represented by a photostationary equilibrium composed of 20% Pr and 80% Pfr (Pratt, 1978) in $H_2O$ upon red-light illumination is profoundly affected by $D_2O$. This report describes a detailed study of these two aspects of phytochrome transformation in $D_2O$.

## Materials and Methods

Undegraded phytochrome was isolated and purified from etiolated oat seedlings (*Avena sativa* L., Garry oats) by a "conventional" method as described earlier (Song et al., 1979) and also by an affinity chromatographic procedure (Smith & Daniels, 1980; Hahn & Song, 1981). In the former, a 4-kg oat seedling tissue extract was successively applied to a brushite column, followed by Sephadex G-25, DEAE-cellulose (Whatman 52) chromatography, and Bio-Gel 0.5 m (Bio-Rad) gel filtration chromatography. Phytochrome preparations of purity indexes ($A_{280}/A_{660}$) ranging from 1.5 to 3.2 were recovered and used.

In the affinity procedure, part of the phytochrome fractionated from brushite chromatography (~20–25 mg) was applied to an Affigel-Blue (Bio-Rad) column equilibrated with 0.1 M potassium phosphate buffer containing 0.1% 2-mercaptoethanol, washed with 0.5 M KCl in the starting buffer, eluted with 10 mM FMN in the starting buffer, and then fractionally precipitated with ammonium sulfate. Phytochrome preparations of purity indexes ranging from 1.2 to 1.8 were recovered after Bio-Gel filtration. No significant differences in spectral behaviors between the conventionally and the affinity-purified phytochromes with different purity indexes were found. Furthermore, phytochrome purified by the immunoaffinity chromatography developed by Hunt & Pratt (1979) showed the same spectral characteristics as those purified by the above two procedures, particularly with regard to the effect of $D_2O$ on the photostationary equilibrium of phytochrome. Thus, unless specified otherwise, data presented in the various figures throughout this report were obtained with the affinity-purified phytochrome. For fluorescence measurements, the affinity-purified phytochrome with a purity index of 1.2 was used exclusively.

$D_2O$ (99.9%) was purchased from Bio-Rad, Oakland, CA. All other chemicals were obtained from Sigma Chemical Co., St. Louis, MO. Deionized distilled water was used to make all buffers and sample solutions in $H_2O$.

† From the Department of Chemistry, Texas Tech University, Lubbock, Texas 79409. *Received January 12, 1981.* This work was supported in part by the Robert A. Welch Foundation (D-182) and the National Science Foundation (PCM79-06806).

0006-2960/81/0420-4315$01.25/0 

Circular dichroic (CD) measurements were carried out at 298 K. All other experiments were done at 277 K under safe green light. Absorption spectral measurements were carried out on a Cary 118C spectrophotometer. Irradiation of phytochrome for assay purposes and for kinetic studies was performed by using a simple accessory for the Cary 118C spectrophotometer (Jung & Song, 1979) combined with either a 660-mm interference filter (Oriel C572-6600) for the red-light source (0.25 $W/m^2$) or an infrared-cutoff filter (Ealing 26-4457) for the far-red light source (40.00 $W/m^2$). For phototransformation kinetic runs, irradiation was carried out by using a Bausch & Lomb microscope illuminator combined with either of the above-mentioned filters (fluence rates 7.5 $W/m^2$ and 1.6 $kW/m^2$ for red and far-red irradiations, respectively). Wavelength dependences of the phototransformation were performed by using a Bausch & Lomb high-intensity monochromator (33-86-07) with a 150-W xenon lamp ($9.3 \times 10^{19}$ quanta $m^{-2}$ $s^{-1}$ at 660 nm).

CD spectra were recorded on a modified JASCO-20 spectropolarimeter as described earlier (Jung et al., 1980). Fluorescence spectra were recorded on a Hitachi Perkin-Elmer spectrofluorometer, Model MPF3. For low-temperature measurements of fluorescence and fluorescence lifetime, a liquid nitrogen optical Dewar was used.

Sample solutions were prepared by precipitating purified phytochrome as freshly isolated in 0.1 M sodium phosphate buffer containing 50 mM KCl, with ammonium sulfate, and then dissolving the pellet in either 0.05 M Tris-$H_2O$ (pH 7.70) or 0.05 M Tris-$D_2O$ (pD 7.69). The concentration of phytochrome used for different sample preparations varied from 0.3 to 4.0 $\mu$M.

Rates of Pr → Pfr phototransformation and Pfr → Pr photoreversion were calculated by plotting the natural logarithms of absorbances at 660 or 725 nm vs. time for the first 20 s. Kinetic parameters for the dark reversion of Pfr to Pr were determined by using the same samples (i.e., immediately prepared phytochrome or recycled samples after red and far-red irradiation cycles), according to the procedure described by Negbi et al. (1975), and the kinetics were then analyzed by the "peeling" procedure to determine the relative proportions of the fast and slow reversion components as described previously (Van Liew, 1967; Hahn & Song, 1981).

## Results

*Effect of $D_2O$ on the Primary Photoprocess.* In analogy to the radiationless process involving proton tunneling in free base porphyrins, the proposed mechanism depicted in Figure 1, which is based on spectroscopic studies of phytochrome (Song et al., 1975, 1979; Song & Chae, 1976), requires that a proton transfer from the ring A nitrogen to the ring C nitrogen take place in competition with the fluorescence emission of the excited singlet ($Q_y$) state of phytochrome (Pr). In support of the mechanism for an intramolecular proton transfer in the excited state, undegraded Pr has an extremely low fluorescence quantum yield and a subnanosecond lifetime at room temperature (Song et al., 1979). From the foregoing, it is anticipated that the fluorescence intensity of phytochrome will be higher in $D_2O$ than in $H_2O$, since deuteron transfer is slower than proton transfer. This prediction is borne out in the data shown in Figure 2. At 277 K, the fluorescence intensity of phytochrome is more than 2-fold higher in $D_2O$ than in $H_2O$. At 77 K, the fluorescence intensity in $D_2O$ is 4 times that in $H_2O$ (e.g., compare the relative intensities of fluorescence excited at 640 nm; Figure 2). Fluorescence excitation spectra of Pr in $D_2O$ and $H_2O$ are also consistent with the emission intensity data (Figure 3). The excitation maxima

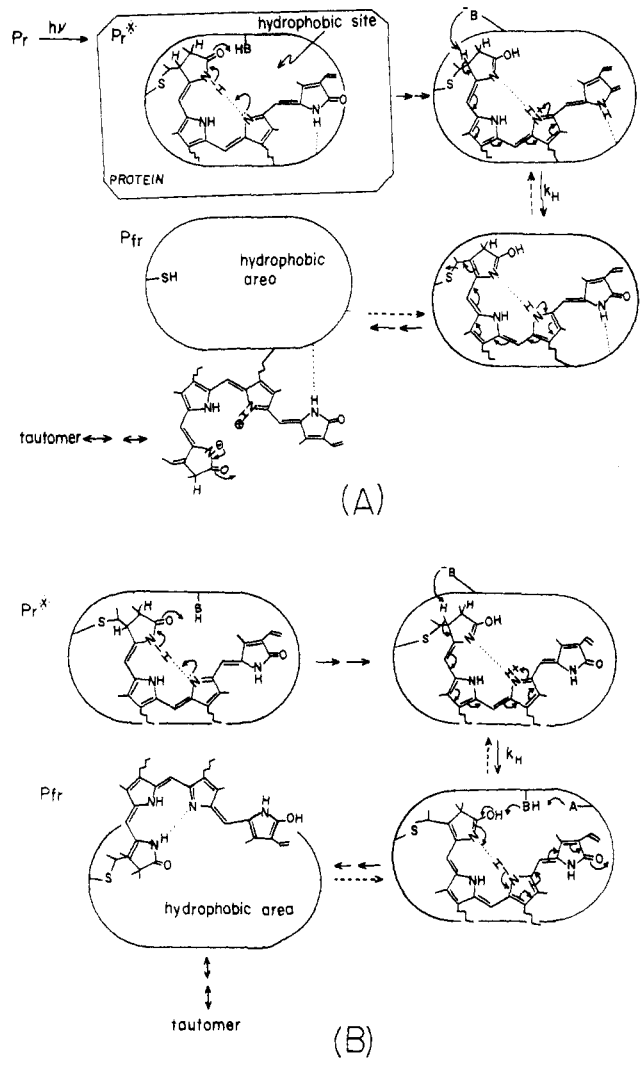


FIGURE 1: Proposed models (top view) for the phototransformation of phytochrome. The essential feature of the models is the development of hydrophobic surface area on the Pfr form as a result of chromophore reorientation with respect to the hydrophobic plane or crevice [modified from Song et al. (1979) and Hahn & Song (1981)]. Model A is based on the release of an additional free -SH group (thioether linkage to ring A) in going from Pr to Pfr and on the assumption that one of the propionic acid side chains (ring C) is covalently linked to the apoprotein [Song et al., 1979; Song, 1980; cf. Killilea et al. (1980)]. Model B is based on the assumption that both propionic acid side chains are free [Hahn & Song, 1981; cf. Lagarias & Rapoport (1980)]. The double arrows after the presumed Pfr structure stand for other tautomeric structures which may also represent the Pfr chromophore. Broken arrows in the reverse direction may represent different mechanistic paths from the forward steps. Dotted line represents hydrogen bonding.

occur at 677 nm in $D_2O$ and at 678 nm in $H_2O$; the red shifts of the excitation maxima relative to the absorption maxima are attributable to the combined effects of the sharpening of band $Q_y$ (Song et al., 1981), the increased dispersion (refractive index) of frozen $D_2O$ and $H_2O$ at 77 K, and the spectral output of the xenon arc intensity, which has a broad peak at 690 nm. Small excitation peaks at 465 nm are also attributable to the xenon output intensity at this wavelength.

*Effect of $D_2O$ on Phototransformation.* As can be seen in Figure 4, 660-nm irradiation of phytochrome (Pr) leads to drastically different photostationary equilibria in $D_2O$ and $H_2O$, which results in a Pfr absorbance at 725 nm that is only half of the 660-nm absorbance in $D_2O$. This effect of $D_2O$ was confirmed with the immunoaffinity purified phytochrome, indicating that the effect observed is independent of the purification method used (spectra not shown). This is important

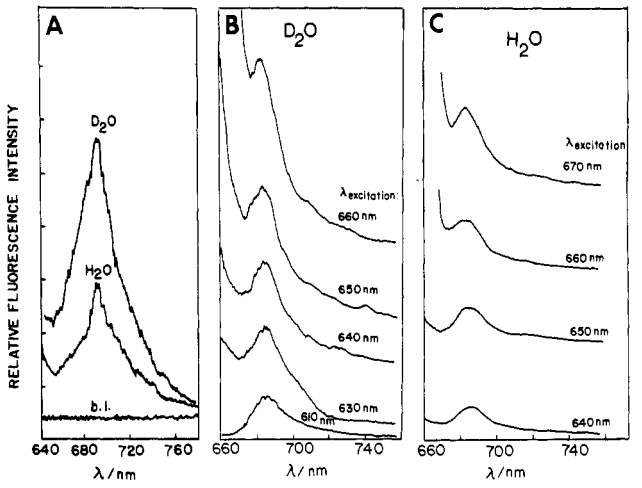


FIGURE 2: (A) Technical fluorescence emission spectra of recycled phytochrome (Pr) in Tris-$D_2O$, pD 7.69, and Tris-$H_2O$, pH 7.70, at 277 K. The 660-nm absorbances of both samples were 0.27. Excitation wavelength, 620 nm; excitation slit, 8 nm; emission slit, 8 nm, b.l. = base-line dark current. (B) Technical fluorescence emission spectra of recycled Pr (absorbance at 660 nm, 0.27 at room temperature) in Tris-$D_2O$, pD 7.69, 77 K. (C) Fluorescence in Tris-$H_2O$, pH 7.70, 77 K. Wavelengths of excitation are indicated. Excitation slit, 2 nm; emission slit, 2 nm.

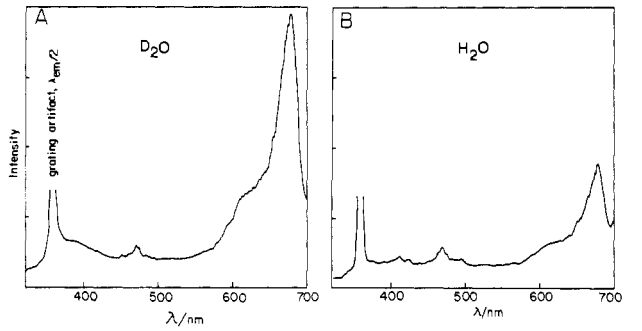


FIGURE 3: Fluorescence excitation spectra of recycled Pr (absorbance, 0.27 at room temperature) in Tris-$D_2O$, pH 7.69 (A), and Tris-$H_2O$, pH 7.70 (B), at 77 K. (A) Emission wavelength monitored, 710 nm; emission band-pass, 3 nm; excitation band-pass, 4 nm. (B) Emission wavelength, 700 nm; emission and excitation band-pass, 3 nm.

to establish, since certain properties of phytochrome, such as solubility and stability, seem to be dependent on the purification methods used.

No gross differences in the absorption spectra were found between the Pr forms of phytochrome dissolved in either $D_2O$ or $H_2O$, in contrast to the difference seen in the photostationary spectra of Pfr. This phenomenon was observed irrespective of whether the spectra of Pr and Pfr were recorded with freshly prepared samples or with solution that had been incubated overnight or longer. However, a closer examination of the absorption spectra of phytochromes in $H_2O$ and $D_2O$ reveals several subtle differences between the two spectra, as illustrated in Figure 5. First, Pr in $D_2O$ absorbs slightly more at wavelengths longer and shorter than 660 nm, whereas Pr in $H_2O$ absorbs slightly more at the 660-nm band. The stronger absorbance at wavelengths below 660 nm for Pr in $D_2O$, relative to Pr in $H_2O$, is also noticeable in Figure 4. This holds true for the wavelength region below the isosbestic point at 683 nm (Figure 5, curve 4). On the other hand, Pfr in $D_2O$ absorbs slightly less than the same form in $H_2O$. This has also resulted in an apparent blue shift of the Pfr absorbance difference maximum, from 715 nm in $H_2O$ to 706 nm in $D_2O$ (compare spectra 2 and 3 in Figure 5).

The circular dichroism spectra of both Pr and Pfr in $D_2O$ and $H_2O$ did not show significant differences, as they fall

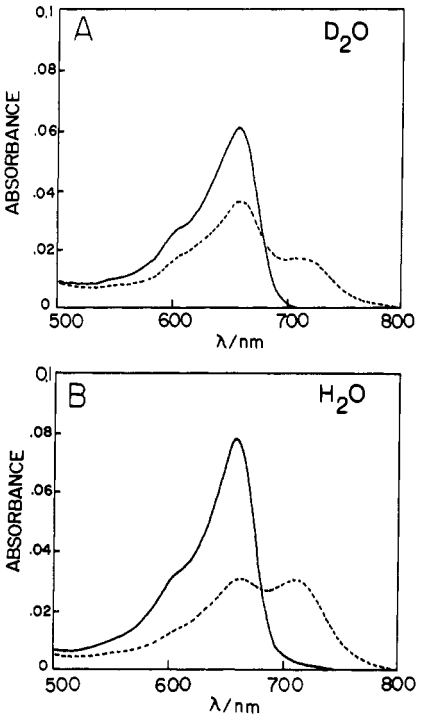


FIGURE 4: Absorption spectra of Pr (solid line) and Pfr (dashed line) in Tris-$D_2O$, pD 7.69 (A), and Tris-$H_2O$, pH 7.70 (B), at 277 K. The photostationary spectra of Pfr were recorded after illumination of Pr with red light, 7.5 W/m$^2$, for 20 min at 277 K. The phytochrome used was purified by the Affi-gel affinity chromatography.

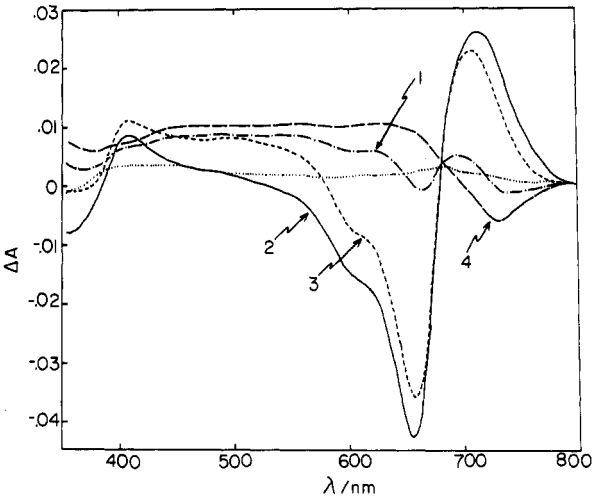


FIGURE 5: Difference spectra of phytochrome in Tris-$D_2O$ (pD 7.20) and Tris-$H_2O$ (pH 7.20). The absorbance of Pr at 660 nm was 0.078. Solutions of Pr in $H_2O$ and $D_2O$ were incubated at 277 K overnight to allow H–D exchange fully in the latter. The actual base line, Pr($H_2O$) vs. Pr($H_2O$), is shown in dotted line. Spectrum 1, Pr($D_2O$) vs. Pr($H_2O$); spectrum 2, Pfr($H_2O$) vs. Pr($H_2O$); spectrum 3, Pfr($D_2O$) vs. Pr($H_2O$); spectrum 4, Pfr($D_2O$) vs. Pfr($H_2O$).

within the range of experimental error inherent in CD measurements (spectra not shown). This was expected from the absorption spectra shown in Figure 4.

Wavelength dependences of the phototransformation from Pr to Pfr were carried out monochromatically in order to explain the $D_2O$ perturbation of the photostationary state of phytochrome. Figure 6 was obtained by plotting either the percent Pfr formed or $\Delta Pfr/\Delta Pr$ as a function of different wavelengths of irradiation for 30 min using a Bausch & Lomb high-intensity monochromator, where $\Delta Pfr$ and $\Delta Pr$ represent the following quantities, respectively:

$$\Delta Pfr = A_{725}^{R} - A_{725}^{FR}$$

$$\Delta Pr = A_{660}^{FR} - A_{660}^{R}$$

Table I[a]

| sample | cycle no. | rate constant ($s^{-1} \times 10^3$) Tris-$H_2O$ | Tris-$D_2O$ | $k_{H_2O}/k_{D_2O}$ |
|---|---|---|---|---|
| Affi-gel purified (immediately prepared sample) | I | 2.45 ($r$ = 0.999) | 2.68 ($r$ = 0.999) | 0.914 |
| | II | 2.38 ($r$ = 0.998) | 2.24 ($r$ = 0.998) | 1.062 |
| | III | 2.24 ($r$ = 0.998) | 2.07 ($r$ = 0.999) | 1.082 |
| | IV | 2.34 ($r$ = 0.999) | 2.00 ($r$ = 0.997) | 1.170 |
| | V | 2.34 ($r$ = 0.999) | 1.85 ($r$ = 0.998) | 1.265 |
| conventional phytochrome (immediately prepared sample) | I | 2.24 ($r$ = 0.998) | 2.25 ($r$ = 0.998) | 0.996 |
| | II | 2.18 ($r$ = 0.991) | 2.20 ($r$ = 0.998) | 0.991 |
| | III | 2.09 ($r$ = 0.999) | 1.95 ($r$ = 0.997) | 1.072 |
| | IV | 2.09 ($r$ = 0.999) | 1.95 ($r$ = 0.997) | 1.072 |
| conventional phytochrome (incubated sample) | I | 2.82 ($r$ = 0.999) | 2.88 ($r$ = 0.998) | 0.979 |
| | II | 2.70 ($r$ = 0.996) | 2.54 ($r$ = 0.996) | 1.063 |
| | III | 2.63 ($r$ = 0.998) | 2.35 ($r$ = 0.996) | 1.120 |

[a] Phototransformation kinetics [Pr → ($h\nu$, 660 nm) Pfr] were measured by monitoring the decay of the 660-nm peak under continuous irradiation, and rate constants were calculated as described under Materials and Methods. The symbol $r$ indicates the correlation coefficient of that measurement. Phytochrome samples were either in Tris-$H_2O$ or in Tris-$D_2O$ buffer (pH = pD ≅ 7.70 at 277 K).

Table II: Decay of the 725-nm Absorbance Peak Monitored To Measure Photoreversion Kinetics from Pfr to Pr[a]

| sample | cycle no. | rate constant ($s^{-1} \times 10^2$) Tris-$H_2O$ | Tris-$D_2O$ | $k'_{H_2O}/k'_{D_2O}$ |
|---|---|---|---|---|
| Affi-gel purified phytochrome without incubation | I′ | 1.48 ($r$ = 0.998) | 1.74 ($r$ = 0.999) | 0.851 |
| | II′ | 1.48 ($r$ = 0.998) | 1.67 ($r$ = 0.997) | 0.886 |
| | III′ | 1.48 ($r$ = 0.998) | 1.85 ($r$ = 0.998) | 0.800 |
| phytochrome from conventional procedure without incubation | I′ | 1.36 ($r$ = 0.996) | 1.37 ($r$ = 0.997) | 0.993 |
| | II′ | 1.40 ($r$ = 0.997) | 1.48 ($r$ = 0.999) | 0.946 |
| | III′ | 1.36 ($r$ = 0.997) | 1.54 ($r$ = 0.999) | 0.883 |
| phytochrome from conventional procedure with incubation and recycling | I′ | 1.73 ($r$ = 0.999) | 1.91 ($r$ = 0.999) | 0.906 |
| | II′ | 1.69 ($r$ = 0.998) | 1.90 ($r$ = 0.998) | 0.889 |
| | III′ | 1.69 ($r$ = 0.998) | 1.90 ($r$ = 0.998) | 0.889 |

[a] Cycle number refers to the sample obtained after photoequilibrium is reached in each respective cycle of the transformation, i.e., Pr → (cycle I, 660 nm) Pfr → (cycle I′, 725 nm) Pr → (cycle II, 660 nm) Pfr → (cycle II′, 725 nm) Pr, etc.

At all wavelengths used, except 690 nm, the amount of Pfr formed is less in $D_2O$ than in $H_2O$. These results were reproducible irrespective of the purity index or the concentration of phytochrome examined. All plots but one show maxima at 660 nm. However, the action maximum of percent Pfr formed is shifted to 670 nm in $D_2O$, relative to that in $H_2O$ (Figure 6).

For quantitative evaluation of the effects of $D_2O$ on the phototransformation of phytochromes, the rates of phototransformation from Pr to Pfr and vice versa were obtained from photokinetic runs. Tables I and II summarize the kinetic results with both conventionally and Affi-gel chromatographically purified phytochromes. The most important finding is the increasing kinetic isotope effect trend in the Pr → Pfr phototransformation in $D_2O$ with each successive cycling of the phytochrome, as predicted in the introduction. However, the isotope effect is not large enough for a rate-determining step involving C–H bond breaking. Furthermore, this rate in $D_2O$ is even slightly faster with an uncycled Pr sample purified by the Affi-gel method (Table I). Similar results were obtained with Affi-gel purified phytochrome dissolved in $H_2O$ and $D_2O$, respectively, and/or by adjusting the pH of the former with NaOH to make pH and pD equal (Table II). However, the reverse phototransformation, Pfr → Pr, shows an inverse isotope effect, as summarized in Tables II and III.

*Effect of $D_2O$ on the Dark Reversion of Pfr.* The Pfr form of phytochrome undergoes dark reversion to the Pr form without far-red illumination. Dark reversion is affected by $D_2O$, as shown in Table IV. Phytochrome solutions in Tris-$D_2O$ always showed more reversion than solutions in Tris-$H_2O$, according to the peeling procedure for resolving the faster component. The decay rate of the fast component is clearly higher in Tris-$D_2O$ than in Tris-$H_2O$. Thus, dark-reversion experiences the $D_2O$ solvent isotope effect somewhat more than does photoreversion (compare the data in Table IV with those in Tables II and III). However, the slower component of dark-reversion kinetics is unaffected by $D_2O$, within experimental error.

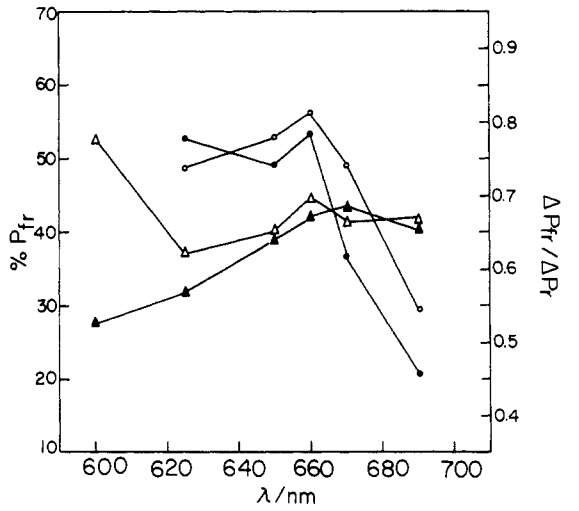


FIGURE 6: Wavelength dependence of Pr–Pfr photostationary equilibrium at 277 K. The phytochrome used was purified by the Affi-gel chromatography. The fluence rates used with a Bausch & Lomb high-intensity monochromator at wavelengths 600, 625, 650, 660, 670, and 690 nm were 0.39, 0.34, 0.40, 0.35, 0.48, and 0.38 W/m$^2$, respectively. The band-pass was set at ~10 nm at each actinic wavelength. Left ordinate: open circle, in $H_2O$, pH 7.56; solid triangle, in $D_2O$, pD 7.60. Right ordinate: solid circle, in $H_2O$, pH 7.56; open triangle, in $D_2O$, pD 7.60. $\Delta Pr = A_{660}^{FR} - A_{660}^{R}$; $\Delta Pfr = A_{725}^{R} - A_{725}^{FR}$.

Table III: Phototransformation Kinetics of Phytochrome[a]

| phototransformation | cycle no. | $k_{a(H_2O)} \times 10^3$, pH 7.10 | $k_{a(H_2O)}/k_{b(D_2O)}$ [b] | $k_{b(D_2O)} \times 10^3$, pD 7.60 | $k_{b(H_2O)} \times 10^3$, pH 7.56 | $k_{b(H_2O)}/k_{b(D_2O)}$ |
|---|---|---|---|---|---|---|
| Pr → Pfr | I | 2.65 ($r$ = 0.988) | 0.89 | 2.99 ($r$ = 0.999) | 3.56 ($r$ = 0.999) | 1.20 |
| | II | 3.08 ($r$ = 0.999) | 1.21 | 2.55 ($r$ = 0.996) | 3.32 ($r$ = 0.998) | 1.30 |
| | III | 3.08 ($r$ = 0.999) | 1.19 | 2.60 ($r$ = 0.999) | 3.11 ($r$ = 0.999) | 1.20 |
| | IV | | | 2.53 ($r$ = 0.999) | 2.99 ($r$ = 0.998) | 1.18 |
| Pfr → Pr | I′ | 25.5 ($r$ = 0.999) | 1.23 | 20.8 ($r$ = 0.999) | 18.4 ($r$ = 0.999) | 0.89 |
| | II′ | 25.0 ($r$ = 0.999) | 1.14 | 22.0 ($r$ = 0.999) | 17.1 ($r$ = 0.999) | 0.78 |
| | III′ | 25.0 ($r$ = 0.999) | 1.17 | 21.4 ($r$ = 0.999) | 17.1 ($r$ = 0.999) | 0.80 |
| | IV′ | | | 22.0 ($r$ = 0.999) | 17.2 ($r$ = 0.998) | 0.78 |

[a] Affi-gel-purified phytochrome was dissolved and incubated overnight in $H_2O$ and $D_2O$. Symbol explanations are same as in Table I. Rate constants in $s^{-1}$. [b] The rate constant subscripts, a and b, stand for pH 7.10 and pH 7.56 or pD 7.60, respectively.

Table IV: Rate Constants for the Pfr → Pr Dark Reversion Resolved by the Peeling Procedure (Tris Buffer)[a]

| | fast component | | | | | slow component | | |
|---|---|---|---|---|---|---|---|---|
| | % amplitude | | $k^0 \times 10^3$ ($s^{-1}$) | | $k^0_{H_2O}/k^0_{D_2O}$ | $k' \times 10^5$ ($s^{-1}$) | | $k'_{H_2O}/k'_{D_2O}$ |
| sample | $H_2O$ | $D_2O$ | $H_2O$ | $D_2O$ | | $H_2O$ | $D_2O$ | |
| Affi-gel purified, without incubation | 22.0 | 26.3 | 1.025 ($r$ = 0.999) | 1.704 ($r$ = 0.997) | 0.60 | 3.330 ($r$ = 0.963) | 3.490 ($r$ = 0.975) | 0.95 |
| Affi-gel purified, incubated and photocycled | 23.0 | 25.5 | 1.081 ($r$ = 0.999) | 1.396 ($r$ = 0.998) | 0.77 | 3.639 ($r$ = 0.976) | 3.838 ($r$ = 0.976) | 0.95 |
| phytochrome from conventional procedure with incubation and photocycling | 17.5 | 24.7 | 1.038 ($r$ = 0.999) | 1.505 ($r$ = 0.999) | 0.69 | 2.197 ($r$ = 0.977) | 2.060 ($r$ = 0.987) | 1.06 |

[a] pH 7.70 and pD 7.69.

## Discussion

It has been shown that undegraded phytochrome (Pr) emits fluorescence that increases in intensity as a function of lowering temperature (Song et al., 1975, 1979). Enhanced fluorescence emission in $D_2O$ was demonstrated in this study, and this enhancement is even more significant at 77 K (Figure 2).[1] These results are consistent with the suggestion that the primary photoprocess of Pr is an intramolecular proton transfer, as illustrated in Figure 1.

The chromophore conformation of Pr is semicircular, and essentially the same conformation is retained in the Pfr chromophore (Song et al., 1979). Such a semicircular conformation allows near copolanarity for the rings A and C, which facilitates proton transfer during the excited-state lifetime. The subnanosecond lifetime is also indicative of the occurrence of a radiationless process (such as the proposed intramolecular proton transfer) with a rate faster than diffusion-controlled processes. As one would expect for an *intramolecular* proton transfer, a 696-nm-absorbing intermediate, arising from the proton transfer, has been detected upon red-light irradiation of Pr at 77 K, suggesting that such an intramolecular proton transfer occurs at low temperatures (Song et al., 1981).

Although the $D_2O$ isotope effect on Pr → Pfr phototransformation increases with the cycling of the phytochrome solutions (Tables I–III), its magnitude is only $\sim 1.3(k_{H_2O}/k_{D_2O})$, suggesting that the rate-limiting step(s) in the Pr → Pfr phototransformation may not involve the dissociation of exchangeable protons. If the proposed mechanism shown in Figure 1 were correct, the C–H bond breaking, $k_H$, is likely to be rate limiting and is thus subject to larger $D_2O$ isotope effects upon cycling the phytochrome in $D_2O$, which was not found to be the case in this study. We cannot rule out the possibilities that the catalytic group involved in step $k_H$ is not fully exposed to the $D_2O$ medium or that some other step in the transformation is rate limiting. However, an adequate account of the observed $D_2O$ effects can be made in terms of either or both of the following explanations.

(a) The Pfr chromophore becomes preferentially more exposed to the medium than does the Pr chromophore, as has been recently shown (Hahn et al., 1980; Hahn & Song, 1981), and thereby one of the N protons (e.g., ring A N–H) in the tetrapyrrole chromophore may be exchanged with deuteron in $D_2O$. Cycling the phytochrome enhances the probability of exchange between the N–H proton and deuteron; the former is likely to be hydrogen bonded to the ring C nitrogen (Figure 1). This could explain the fluorescence enhancement in $D_2O$.

(b) One or more specific amino acid residues are involved at the catalytic site in phototransformation. Hunt & Pratt (1981) recently suggested the possible involvement of two tyrosyl residues in the phototransformation of phytochrome by demonstrating the complete loss of photoreversibility for both Pr and Pfr upon modification of these residues with tetranitromethane. We propose that tyrosyl hydroxyl protons act as a general acid catalyst (as opposed to a specific acid catalyst) and that the isotope effect observed after cycling then results from the increasing H–D exchange between the tyrosyl hydroxyl group(s), as the general acid, Tyr-O*D*, participates in a partially or non-rate-limiting step.

Kendrick & Spruit (1972) observed that in a $D_2O$–phosphate buffer at 0 °C the amount of phytochrome intermediates that accumulate under conditions of photocycling is greater than in $H_2O$. This was subsequently explained by considering that the rate of the dark reaction of meta-Rb to Pfr is slower in $D_2O$ than in $H_2O$ (Kendrick & Spruit, 1976). This would partly explain the observed displacement of the photostationary state of phytochromes in $D_2O$ (Figure 4). The observed shift in the action spectrum maximum (Figure 6) may be due to

[1] The fluorescence intensity enhancement in $D_2O$ increases with recycling of phytochrome (Pr → Pfr → Pr →, etc.) in $D_2O$, suggesting that the recycling exposes chromophore to the medium for N–H and $D^+$ exchanges. At 292 K, the fluorescence lifetimes were 0.14 and 0.29 ns in Tris-$H_2O$ and Tris-$D_2O$, respectively. Relatively high absorbances ($\sim$0.23) were required for these measurements because of extremely low fluorescence quantum yields at room temperature (Song et al., 1975).

the diminished Pfr formation upon irradiation with 660-nm light, as compared to the decrease in the Pr form. Indeed, the difference spectrum of Pr in $D_2O$ vs. Pr in $H_2O$ suggests a slightly less absorption at 660 nm for the former (Figure 5). Additionally, the molar extinction coefficient of the $Q_x$ band of Pfr (~660 nm) is stronger in $D_2O$ than in $H_2O$, which could account for the displacement of photostationary equilibrium. However, what fraction of the positive absorbance difference at 660 nm in spectrum 4 (Figure 5) is contributed to by the molar extinction difference cannot be estimated quantitatively, since a full spectrum of 100% Pfr solution is not available. It appears that several factors contribute to the shift in the photostationary state of phytochromes in $D_2O$. These include (a) a lower molar extinction coefficient of the Pr $Q_y$ band at 660 nm in $D_2O$ than in $H_2O$, vide supra, (b) a possibly higher molar extinction of the Pfr $Q_x$ band at 660 nm in $D_2O$ than in $H_2O$, vide supra, and (c) the faster photoreversion and dark reversion of Pfr, combined with the slower photoconversion of Pr in $D_2O$ than in $H_2O$ (cf. Tables I–IV).

The rate of photoreversion in small or degraded phytochrome, which behaves photochemically similar to undegraded phytochrome (Pratt & Cundiff, 1975; Pratt, 1978), is independent of pH over the range 6.9–8.6, but the rate is accelerated on lowering the pH below 6.0 (Mumford et al., 1968; Anderson et al., 1969). These observations and the data presented in Table III are consistent with the idea of an acid-catalyzed reaction for the photoreversion, in which histidyl residue with a $pK_a$ of 6.5 (Song et al., 1979) or carboxyl residue with a relatively high $pK_a$ in a hydrophobic environment may act as the conjugate acid in protonating Pfr to $PfrH^+$ (or $PfrD^+$ in $D_2O$). However, it would be premature to state whether the reaction is specific-acid (hydronium or deuteronium ion) or general-acid catalyzed until a systematic photokinetic study, as a function of buffer concentration, is carried out. An observed solvent isotope effect of less than the theoretically predicted value of 3.6 (Wiberg, 1964) is explainable in terms of the partial shielding of catalytic residue(s) from the medium, multistep reactions involving the chromophore and apoprotein, and the fact that photoreactions occurring from excited, metastable state potential surfaces often do not produce large isotope effects.

The dark-reversion kinetics of Pfr is biphasic in aqueous solution (Negbi et al., 1975; Taylor, 1968; Boisard et al., 1970; Manabe & Furuya, 1971; Pike & Briggs, 1972). Recently, we proposed a consecutive kinetic model for the biphasic decay of Pfr (Hahn & Song, 1981):

$$\mathrm{Pfr} \underset{\text{fast}}{\overset{k_{-1}}{\rightarrow}} \mathrm{Pfr}' \underset{\text{slow}}{\overset{k_{-2}}{\rightarrow}} \mathrm{Pr}, \text{ etc.}$$

The present results on dark-reversion kinetics show an increase in both amplitude and rate of the faster component (Table IV). This can be accommodated in terms of the above scheme. Further support for this scheme comes from the data shown in Table III where, because of the difference in pH and pD, the rate of photoreversion is faster in $H_2O$ than in $D_2O$.

## Acknowledgments

We thank Professor L. H. Pratt and Dr. W. O. Smith for their helpful suggestions regarding the immunoaffinity and Affi-gel affinity chromatographic procedures, respectively.

## References

Anderson, G. R., Jenner, E. L., & Mumford, F. F. (1969) *Biochemistry 8*, 1182–1187.

Boisard, J., Marmé, D., & Schäfer, E. (1970) *Planta 99*, 302–310.

Hahn, T.-R., & Song, P. S. (1981) *Biochemistry 20*, 2602–2609.

Hahn, T.-R., Kang, S.-S., & Song, P. S. (1980) *Biochem. Biophys. Res. Commun. 97*, 1317–1323.

Hunt, R. E., & Pratt, L. H. (1979) *Plant Physiol. 64*, 332–336.

Hunt, R. E., & Pratt, L. H. (1981) *Biochemistry 20*, 941–945.

Jung, J., & Song, P. S. (1979) *Photochem. Photobiol. 29*, 419–421.

Jung, J., Song, P. S., Paxton, R. J., Edelstein, M. S., Swanson, R., & Hazen, E. E., Jr. (1980) *Biochemistry 19*, 24–32.

Kendrick, R. E., & Spruit, C. J. P. (1972) *Plant Physiol. 52*, 327–331.

Kendrick, R. E., & Spruit, C. J. P. (1976) in *Light and Plant Development* (Smith, H., Ed.) pp 31–43, Butterworths, London.

Killilea, S. D., O'Carra, P., & Murphy, R. F. (1980) *Biochem. J. 187*, 311–320.

Klein, G., & Rüdiger, W. (1978) *Liebigs Ann. Chem. 2*, 267–279.

Lagarias, J. C., & Rapoport, H. (1980) *J. Am. Chem. Soc. 102*, 4821–4828.

Manabe, K., & Furuya, M. (1971) *Plant Cell Physiol. 12*, 95–101.

Mumford, F. E., Anderson, G. R., & Jenner, E. L. (1968) *Plant Physiol. (Suppl.) 43*, S-15.

Negbi, M., Hopkins, D. W., & Briggs, W. R. (1975) *Plant Physiol. 56*, 157–159.

Pike, C. S., & Briggs, W. R. (1972) *Plant Physiol. 49*, 514–520.

Pratt, L. H. (1978) *Photochem. Photobiol. 27*, 81–105.

Pratt, L. H., & Cundiff, S. C. (1975) *Photochem. Photobiol. 21*, 91–98.

Rüdiger, W. (1980) *Struct. Bonding (Berlin) 41*, 101–141.

Smith, W. O., & Daniels, S. (1980) *Plant Physiol. (Suppl.) 65*, S-2.

Song, P. S. (1980) in *Photoreception and Sensory Transduction in Aneural Organisms* (Lenci, F., & Colombetti, G., Ed.) pp 235–240, Plenum Press, New York.

Song, P. S., & Chae, Q. (1976) *J. Lumin. 12*, 831–837.

Song, P. S., & Chae, Q. (1979) *Photochem. Photobiol. 30*, 117–123.

Song, P. S., Chae, Q., & Briggs, W. R. (1975) *Photochem. Photobiol. 22*, 74–75.

Song, P. S., Chae, Q., & Gardner, J. G. (1979) *Biochim. Biophys. Acta 576*, 479–495.

Song, P. S., Sarkar, H. K., Kim, I. S., & Poff, K. L. (1981) *Biochim. Biophys. Acta 635*, 369–382.

Taylor, A. O. (1968) *Plant Physiol. 43*, 767–774.

Van Liew, H. D. (1967) *J. Theor. Biol. 16*, 43–53.

Wiberg, K. (1964) *Physical Organic Chemistry*, pp 273–277, Wiley, New York.